



## Molecular Crystals and Liquid Crystals Incorporating Nonlinear Optics

Publication details, including instructions for authors and  
subscription information:

<http://www.tandfonline.com/loi/gmcl17>

### Structures and Mechanisms of Phase Transitions in Surfactant Mixtures: Systems Which Induce the Ribbon Phase

L. J. Lis<sup>a</sup>, P. J. Quinn<sup>b</sup> & J. M. Collins<sup>c</sup>

<sup>a</sup> Department of Physics and The Liquid Crystal Institute, Kent  
State University, Kent, OH, 44242

<sup>b</sup> Department of Biochemistry, King's College London, Kensington  
Campus, London, W8 7AH, U.K.

<sup>c</sup> Department of Physics, Marquette University, Milwaukee, WI,  
53233

Version of record first published: 04 Oct 2006.

To cite this article: L. J. Lis, P. J. Quinn & J. M. Collins (1989): Structures and Mechanisms of  
Phase Transitions in Surfactant Mixtures: Systems Which Induce the Ribbon Phase, *Molecular  
Crystals and Liquid Crystals Incorporating Nonlinear Optics*, 170:1, 119-133

To link to this article: <http://dx.doi.org/10.1080/00268948908047753>

PLEASE SCROLL DOWN FOR ARTICLE

Full terms and conditions of use: <http://www.tandfonline.com/page/terms-and-conditions>

This article may be used for research, teaching, and private study purposes. Any  
substantial or systematic reproduction, redistribution, reselling, loan, sub-licensing,  
systematic supply, or distribution in any form to anyone is expressly forbidden.

The publisher does not give any warranty express or implied or make any  
representation that the contents will be complete or accurate or up to date. The  
accuracy of any instructions, formulae, and drug doses should be independently  
verified with primary sources. The publisher shall not be liable for any loss, actions,  
claims, proceedings, demand, or costs or damages whatsoever or howsoever caused  
arising directly or indirectly in connection with or arising out of the use of this material.

# Structures and Mechanisms of Phase Transitions in Surfactant Mixtures: Systems Which Induce the Ribbon Phase

L. J. LIS

*Department of Physics and The Liquid Crystal Institute, Kent State University, Kent, OH 44242*

and

P. J. QUINN

*Department of Biochemistry, King's College London, Kensington Campus, London, W8 7AH, U.K.*

and

J. M. COLLINS

*Department of Physics, Marquette University, Milwaukee, WI 53233*

*(Received October 1, 1988; in final form October 20, 1988)*

Phase transitions in lyotropic liquid crystal systems made from potassium palmitate/potassium laurate/water (KP/KL/H<sub>2</sub>O) and potassium palmitate/benzoyl alcohol/water (KP/BZA/H<sub>2</sub>O) were characterized by time resolved x-ray diffraction done at the SERC Daresbury (U.K.) Synchrotron Laboratory. Hysteretic phase behavior was observed for some of the KP/KL/H<sub>2</sub>O mixtures but not for any of the KP/BZA/H<sub>2</sub>O mixtures studied. In addition, the transition between the rectangular and ribbon phases in these systems is described using x-ray diffraction. General trends related to the observation of phase transitions in these systems are discussed. The ribbon phase appears to be more stable in the KP/BZA/H<sub>2</sub>O system since it retains its structure after the coexisting lamellar phase has transformed into a liquid crystalline bilayer for a larger temperature range than for KP/KL/H<sub>2</sub>O.

## INTRODUCTION

The presence of a variety of lyotropic liquid crystal phases in surfactant systems is well documented.<sup>1,2</sup> The phases can differ in their mesophase (three dimensional) structure<sup>1</sup> or in the packing of the hydrocarbon moieties within a (two-dimensional) subcell.<sup>1</sup> Typical mesophase structures include the multi-bilayer array and hexagonal array of cylinders. The hydrocarbon chains can pack in hexagonal subcells for the gel ( $L_\beta$  or  $L_{\beta'}$ ), quasi-liquid like packing for the liquid crystalline ( $L_\alpha$ ,  $H_\alpha$ ) classifications, and in more closely packed arrays for the "crystalline" or subgel classification.

One of the more interesting phases formed in surfactant systems is the rectangular array of cylinders.<sup>1</sup> It has been hypothesized<sup>3</sup> that this array is an intermediate resulting from the axial growth of the cylindrical phase in the lamellar to hexagonal phase transition (i.e., the intermediate region). A rectangular phase consisting of non-circular cylinders (the ribbon phase) has also been inferred by NMR measurements in mixtures of potassium palmitate (KP) and potassium laurate (KL) in water<sup>4-7</sup> based on the reported structural analysis in the sodium decylsulphate/1-decanol/H<sub>2</sub>O system.<sup>8</sup> The ribbon phase has been shown in a number of ternary KP/KL/H<sub>2</sub>O mixtures to coexist over some temperature range with either a gel state or liquid crystal bilayer phase.<sup>4-7</sup> These NMR measurements are also clear in establishing the segregation of KL into the curved portions of the ribbon.

It has become apparent that for both surfactants and their biological analog lipids when dispersed in water, there is a temporal hysteresis on cooling between the liquid crystalline or fluid phase and the stable low temperature crystalline phase.<sup>9-15</sup> This hysteresis requires from hours to days for the transition to the subgel phase to go to completion and is a function of the temperature at which the sample is incubated. We have also recently shown that an  $L_C$  phase can be induced for perdeuterated potassium palmitate in D<sub>2</sub>O.<sup>15</sup> Upon continuous heating, transformations involving at least two gel and two liquid crystalline phases were observed. These transformations involved the continuous distortion of the initial subgel acyl chain packing and may indicate that the transformations are second order. Upon cooling, the hysteretic formation of a gel state bilayer occurs.

In this report, the changes in the mesophase structures and acyl chain packing with dynamic changes in temperature for mixtures of potassium palmitate/potassium laurate/water, and potassium palmitate/benzoyl alcohol/water are described. Transitions between phases are also described in relation to their influence on the diffraction patterns produced by the system. High resolution x-ray diffraction patterns have also been obtained for the initial low temperature, high temperature and final low temperature phases. Hysteresis in these systems can now be described relative to changes in the appropriate x-ray diffraction patterns and include information of subgel and gel state hydrocarbon chain packing phases.

## MATERIALS AND METHODS

Mixtures were prepared by weighing and mixing components in a glass tube which was subsequently sealed under a nitrogen atmosphere. Homogenization of the samples was reached by alternately heating and centrifuging the samples. The samples were then refrigerated overnight and allowed to equilibrate for at least five days at room temperature to insure the formation of the crystalline hydrocarbon subcell.

X-ray diffraction patterns were obtained using the 0.150 nm x-radiation at station 7.2/3 of the synchrotron radiation source at the SERC Daresbury Laboratory.<sup>16</sup> A cylindrically bent single crystal of Ge<sup>17</sup> and a long float-glass mirror were used for monochromatization and horizontal focusing, providing about  $2 \times 10^9$  photons  $\cdot$  s<sup>-1</sup> down a 0.2 mm colimator at a 2.0 GeV and 200 to 30 mA of electron

beam current. A Keele flat-plate camera was used with a sample path of 1 mm. Sample temperature was controlled by water baths connected internally to the sample mount of the x-ray camera. Scattered x-rays were recorded on a linear detector constructed at the Daresbury Laboratory. The dead time between continuous data acquisition frames was 50  $\mu$ s with the temporal resolution of each frame of 1.2 s. Individual diffraction patterns were also collected over 100 s. X-ray scattering has been plotted as a function of reciprocal space,  $s = 2 \sin\theta/\lambda$ , using software available at the Daresbury Laboratory. Teflon ( $1/s = 0.48$  nm) was used as a calibration standard for our detection system to convert channel numbers of the linear detector into values of  $s$ . All mesophase and subcell spacings were calculated using Bragg's law.<sup>19</sup> The use of a flat camera introduces diffraction peak distortions which preclude a detailed analyses of the structural parameters determined for the various systems.

## RESULTS

The mesophase and subcell repeat spacings were determined from static x-ray patterns for mixtures of potassium palmitate (KP)/potassium laurate (KL)/water ( $H_2O$ ) and potassium palmitate (KP)/benzoyl alcohol (BZA)/water ( $H_2O$ ) at a) ca. 20°C after extensive equilibration at room temperature, b) ca. 70°C after heating at 10°C/min. and c) ca. 10°C after being cooled at 10°C/min. Summaries of our findings are listed in Tables I and II for KP/KL/ $H_2O$  and KP/BZA/ $H_2O$ , respectively. Each high resolution pattern had from 10 to 15 repeat spacings. In our analysis, we were guided by the previous NMR phase characterization of these systems done by Doane and co-workers.<sup>4-7</sup> In particular, Doane and co-workers<sup>4-7</sup> showed that both systems produced rectangular and ribbon mesophases which typically coexisted with a lamellar phase. The acyl chain packing within these mesophases was determined from an examination of the order parameters of the methylene groups along the length of the acyl chain. The rectangular and ribbon phases were found to contain liquid crystalline (or disordered) state hydrocarbon chains, while a gel to liquid crystalline transition was observed in the coexisting lamellar phase. We were able to differentiate the repeat sequences for the rectangular phase axes, and any additional lamellar phase by our observation of an additional repeat sequence which could be correlated to the diffraction from the diagonal direction within the rectangular array of cylinders. These repeat spacings represent planes perpendicular to the diagonal of the rectangular unit cell. The  $d$ -spacings for these planes are related to the  $a$  and  $b$  axes of the rectangular unit cell by the formula:

$$\frac{1}{d^2} = \frac{h^2}{a^2} + \frac{k^2}{b^2}$$

where  $h$  and  $k$  are the Miller's indices for the plane. The camera used in these studies was positioned such that diffraction lines from repeat spacings of ca. 10.0 nm and lower would be observed. Classification of the acyl chain subcell of the lamellar phase was done by correlating the number of repeat spacings to the number

TABLE I

Summary of structural determinations via x-ray diffraction for mixtures of potassium palmitate (KP)/potassium laurate (KL)/water. The temperature sequence is as follows: initial pattern, pattern after heating and pattern after cooling

Sample	Mixture (wt%)			Temperature °C	Mesophase <i>d</i> -spacings	Acyl chain subcell spacings
	KP	KL	H <sub>2</sub> O			
1	59.8	7.8	32.4	19°	Lamellar 7.07 nm	Monoclinic 0.467, 0.399, 0.36 nm
					Rectangular 4.46, 3.28 nm	(Disordered 0.449 nm)
				64°	Lamellar 3.81 nm	Disordered 0.449 nm
				8°	Lamellar 7.07 nm	Hexagonal 0.391 nm
2	45.1	22.8	32.1		Rectangular 5.05, 4.23 nm	(Disordered 0.449 nm)
				22°	Lamellar 7.07 nm	Orthorhombic 0.412, 0.394 nm
					Rectangular 4.32, 3.87 nm	(Disordered 0.449 nm)
				70°	Lamellar 3.9 nm	Disordered 0.449 nm
3	28.4	40.0	31.6	15°	Lamellar 7.07 nm	Orthorhombic 0.412, 0.397 nm
					Rectangular 4.951, 3.84 nm	(Disordered 0.449 nm)
				25°	Lamellar 7.39 nm	Orthorhombic 0.412, 0.394 nm
					Rectangular 5.21, 4.06 nm	(Disordered 0.449 nm)
4	11.1	56.1	32.8	80°	Lamellar 4.06 nm	Disordered 0.449 nm
				16°	Lamellar 7.07 nm	Orthorhombic 0.399, 0.354 nm
					Rectangular 3.67, 2.75 nm	(Disordered 0.449 nm)
				24°	Lamellar 7.07 nm	Orthorhombic 0.412, 0.391 nm
					Rectangular 5.32, 3.62 nm	(Disordered 0.449 nm)
					Lamellar 7.28 nm	Orthorhombic 0.414, 0.368 nm
					Rectangular 5.5, 3.59 nm	(Disordered 0.449 nm)

TABLE II

Summary of structural determinations via x-ray diffraction for mixtures of potassium palmitate (KP)/benzoyl alcohol (BZA)/water. The low and high temperature structures are defined

Sample	Mixture (wt%)			Temperature °C Mesophase <i>d</i> - spacings	Acyl chain subcell spacings	
	KP	BZA	H <sub>2</sub> O			
B2	66.5	1.1	32.4	24°	(Lamellar 6.35 nm) Rectangular 6.35, 3.96 nm	Monoclinic 0.462, 0.398, 0.56 nm (Disordered 0.45 nm)
				80°	Lamellar 4.13 nm	Disordered 0.45 nm
				28°	(Lamellar 5.54 nm) Rectangular 5.54, 4.14 nm	Monoclinic 0.464, 0.398, 0.356 nm (Disordered 0.45 nm)
B3	65.9	2.1	32.0	80°	Lamellar 4.0 nm	Disordered 0.45 nm
				26°	(Lamellar 5.54 nm) Rectangular 5.54, 4.14 nm	Monoclinic 0.46, 0.386, 0.354 nm (Disordered 0.45 nm)
				80°	Lamellar 3.87 nm	Disordered 0.45 nm

of diffraction directions within a subcell.<sup>20</sup> Representative patterns are shown in Figures 1 and 2. Sequences of repeat spacings for both rectangular axes, the diagonal planes and an independent lamellar phase could be assigned for the KP/KL/H<sub>2</sub>O mixtures at low temperatures, while sequences for the rectangular axis and the diagonal planes could be assigned for the KP/BZA/H<sub>2</sub>O mixtures at low temperatures. Tables III and IV show an analysis of the mesophase diffraction planes for the patterns on Figures 1 and 2. The acyl chain diffraction peaks for the liquid crystalline chain packing of the rectangular or ribbon phases can be inferred to be a disordered subcell with a dimension of 0.449 or 0.450 nm in all systems.

There is no apparent hysteresis observed in any of the KP/BZA/H<sub>2</sub>O mixtures. All three mixtures returned to the same mesophase and lamellar acyl chain subcell structures after heating and cooling at 10°C min<sup>-1</sup> as were observed before heating. The rectangular phases have approximately the same axial dimensions for all three mixtures and the lamellar acyl chains pack in a monoclinic subcell. The high temperature phase in all three mixtures consists of lamellae with disordered acyl chains (i.e.,  $L_a$ ) packed in a liquid crystalline array with a  $d$ -spacing of 0.45 nm which is similar to that observed for KP/D<sub>2</sub>O mixtures.<sup>15</sup> The low temperature lamellar subgel phase, however, has a different acyl chain packing than that observed for

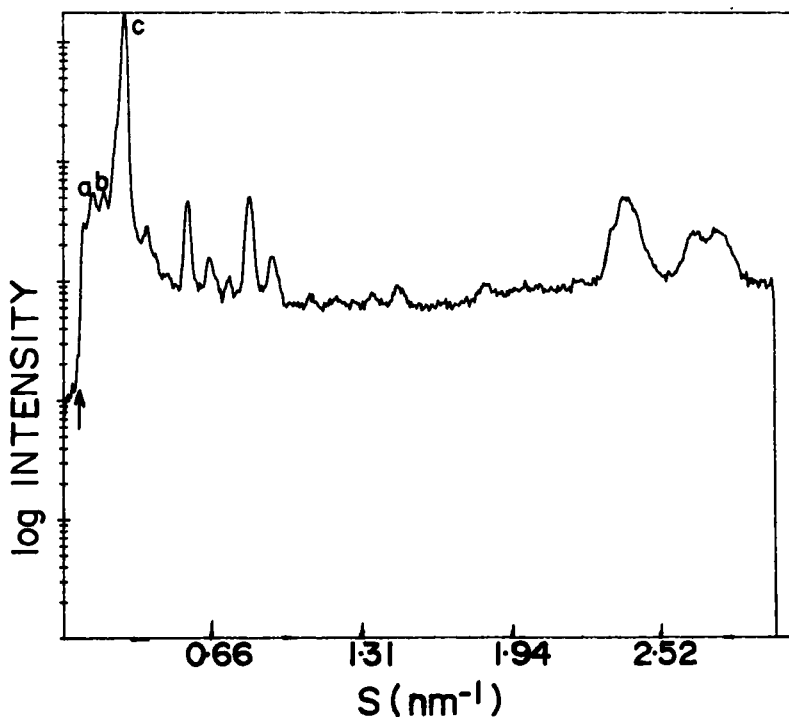


FIGURE 1 X-ray diffraction pattern plotted as log intensity versus reciprocal spacing for a mixture of potassium palmitate/potassium laurate/water of 11.1%/56.1%/32.8% by weight obtained at 24°C. The first order reflections assigned to the 7.09 nm lamellar repeat spacing, and the 5.32 and 3.62 nm rectangular phases axes are indicated by the letters a, b and c, respectively. An arrow marks the spatial limitation due to the beam stop in this diffraction pattern.

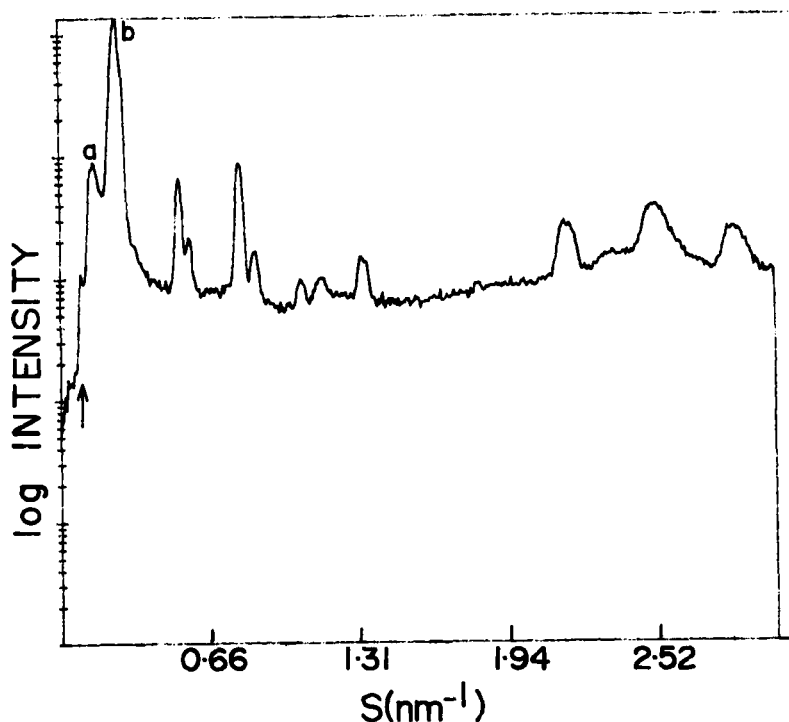


FIGURE 2 X-ray diffraction pattern plotted as log intensity versus reciprocal spacing for a mixture of potassium palmitate/benzoyl alcohol/water of 66.5%/1.1%/32.4% by weight obtained at 24°C. The first order reflections assigned to lamellar or planar arrays of dimension 6.35 and 3.96 nm are designated by the letters a and b, respectively. An arrow marks the spatial limitation due to the beam stop in this diffraction pattern.

KP in D<sub>2</sub>O.<sup>15</sup> This may be due to the difference in solvents used. However, our results provide unambiguous evidence for the retention of a lamellar subgel phase in these mixtures. One could also hypothesize that the perturbation caused by BZA is minimal in the KP cylindrical packing. We observe no additional reflections that can be attributed to a multilamellar phase. However, we can assume that an independent lamellar phase is present with similar dimensions to either of the axes of the rectangular array of cylinders<sup>21</sup> since acyl chain reflections other than for a liquid crystalline phase were observed. On the basis of our previous studies of perdeuterated KP we can infer that the lamellar repeat is that of the larger rectangular axis (Table II).

Mixtures of KP/KL/H<sub>2</sub>O were less consistent in their hysteretic behavior. Mixtures A2 and A4 showed essentially no hysteretic behavior in terms of mesophase or lamellar acyl chain subcell packing structure. All dimensions were equivalent before and after the thermal cycle for sample A2 and only one dimension of the lamellar acyl chain subcell changed for sample A4. Sample A1 showed hysteresis in the lamellar acyl chain packing structure. The lamellar acyl chains in this mixture packed in an hexagonal two-dimensional array after the thermal cycle, whereas the initial subcell was in a subgel or crystalline array. Mixture A3 showed hysteresis



TABLE III  
Assignment of  $(h,k)$  reflections for static x-ray pattern shown in Figure 1

Mesophase	$h$	$k$	$d_{\text{obs}}$ (nm)	$d_{\text{calc}}$ (nm)
Rectangular	1	0	5.32	5.32
	0	1	3.62	3.62
	1	1	2.98	2.99
	2	0	2.63	2.66
	2	1	2.14	2.14
	0	2	—	1.81
	3	0	1.77	1.77
	1	2	—	1.71
	1	3	—	1.65
	3	1	—	1.59
	2	2	1.52	1.50
	4	0	1.31	1.33
	3	2	—	1.27
	4	1	—	1.25
	0	3	1.19	1.21
	2	3	—	1.10
	4	2	—	1.07
	5	0	—	1.06
	3	3	0.98	1.00
	0	4	—	0.91
	4	3	—	0.89
	1	4	—	0.89
	6	0	—	0.89
	2	4	—	0.86
	3	4	0.81	0.81
	7	0	0.77	0.76
	4	4	0.77	0.75
	0	5	0.72	0.72
	8	0	0.66	0.67
	0	6	—	0.60
Lamellar	1	0	7.07	7.07
	2	0	3.62	3.53
	3	0	2.42	2.36
	4	0	1.77	1.77
	5	0	1.45	1.41
	6	0	1.16	1.18

in the mesophase structure and subcell dimensions. The lowest temperature mesophase structures were consistent with being coexistent rectangular and lamellar phases. This sample showed a decrease in both the mesophase and subcell dimensions after heating and cooling. In all mixtures only a single lamellar phase with disordered acyl chains (wide angle diffraction spacing 0.45 nm) were observed at the highest temperatures studied. We can again hypothesize that the presence of KL has a minimal perturbation on the acyl chain packing of the KP molecules in the cylinder or bilayer. Although the lamellar subcell packing is different than that observed for KP in  $\text{D}_2\text{O}$ , there is not enough disruption of the lamellar acyl chain packing to allow for the creation of a gel phase (i.e., ordered hexagonal subcell) rather than a sub-gel phase.

TABLE IV

Assignment of  $(h,k)$  reflections for static x-ray pattern shown in Figure 2

Mesophase	$h$	$k$	$d_{\text{obs}}$ (nm)	$d_{\text{calc}}$ (nm)
Rectangular	1	0	6.35	6.35
	0	1	3.96	3.96
	1	1	—	3.36
	2	0	3.14	3.18
	2	1	—	2.48
	3	0	—	2.12
	0	2	—	1.98
	1	2	1.90	1.89
	3	1	1.90	1.89
	2	2	1.72	1.68
	4	0	—	1.59
	3	2	—	1.45
	4	1	—	1.47
	0	3	—	1.32
	1	3	—	1.29
	5	0	—	1.27
	4	2	1.24	1.24
	2	3	—	1.22
	3	3	1.14	1.12
	6	0	—	1.06
	4	3	—	1.02
	0	4	—	0.99
	1	4	—	0.98
	2	4	—	0.95
	7	0	0.92	0.91
	3	4	—	0.90
	4	4	0.85	0.84
	0	5	—	0.79
	8	0	—	0.79
	9	0	0.73	0.71
	0	6	—	0.66
Lamellar	1	0	6.35	6.35
	2	0	3.14	3.18

Time-resolved x-ray diffraction measurements were obtained for each of these mixtures. As the samples were heated or cooled at  $10^{\circ}\text{C min}^{-1}$  x-ray diffraction patterns of 1.2 s duration were recorded for a total of 255 frames. The diffraction patterns were analyzed to determine mesophase and lamellar subcell dimensions and structures or packing arrays. Only the heating scans are described since there was hysteresis on cooling in the KP/KL/ $\text{H}_2\text{O}$  systems but not the KP/BZA/ $\text{H}_2\text{O}$  samples.

An examination of these continuously-recorded diffraction patterns indicate that the transitions in the KP/KL/ $\text{H}_2\text{O}$  system are unaffected by the change in mole ratio of KP/KL. One would expect that the presence of increasing amounts of KL would tend to cause a disordering of the lamellar acyl chain packing and perhaps a lowering of the various transition temperatures. The diffraction patterns collected during the heating cycle for sample A4 are shown in Figure 3. The transition from

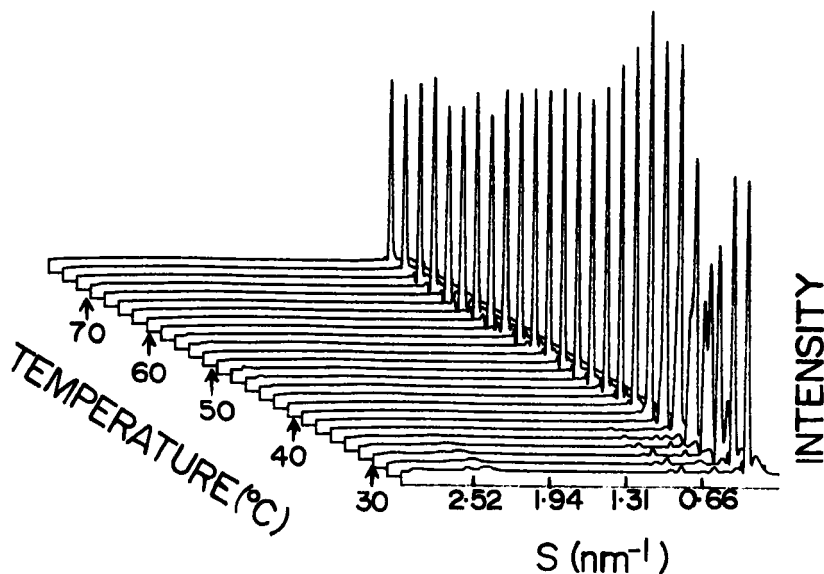
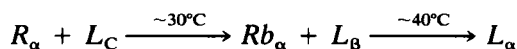


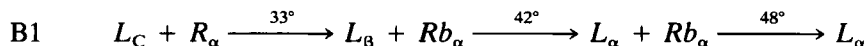
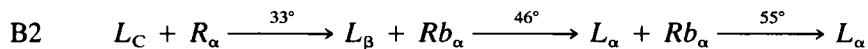
FIGURE 3 X-ray diffraction patterns of a 11.1%/56.1%/32.8% mixture by weight of potassium palmitate/potassium laurate/H<sub>2</sub>O collected every 1.2 s as the sample is heated by 10°C min<sup>-1</sup>. The intensity is plotted as a function of reciprocal spacing. Every tenth frame in the data set is shown in this figure.

the crystalline (monoclinic or orthorhombic) subcell to an hexagonal array of ordered acyl chains (referred to as the  $\beta$  phase) in the lamellar phase preceded in temperature a transition from the rectangular to the ribbon array (i.e., flattened cylinders packed rectangularly). This interpretation is consistent with previous NMR observations.<sup>4-7</sup> The acyl chain order within the lamellar mesophases has been previously shown<sup>5-7</sup> to be the same in the ordered hexagonal and disordered subcells. It has also been conclusively<sup>4-7</sup> shown that KL diffuses to the curved regions of the ribbon and disorders the KP molecular packing. From our present studies, we can infer that this perturbation probably does not extend to the flat portions of the ribbon or the independent lamellar phase. The transformation to the ribbon phase was thus indicated by the loss of higher order x-ray diffraction peaks from the rectangular array. No dimensional change in the  $a$  and  $b$  axes was observed during these transitions. The further disordering of the lamellar acyl chain subcell (referred to as the  $\alpha$  phase) resulted in the two phase system transforming into a single lamellar phase. The transformation scheme in terms of mesophase structure and acyl chain packing subcell observed for these mixtures is



where  $R$  is the rectangular phase,  $Rb$  the ribbon phase,  $L$  the lamellar phase, and  $C$ ,  $B$  and  $\alpha$  referred to different acyl chain subcells. The transformation between the rectangular and ribbon phases was indicated by a decrease in the intensity of the higher order mesophase scattering peaks. There is no apparent change in the mesophase dimensions during this transition.

An examination of the x-ray diffraction patterns recorded while mixtures of KP/BZA/H<sub>2</sub>O underwent heating and cooling showed a less uniform behavior. The indexing of the mesophase and subcell diffraction peaks indicated the following transformation schemes for these KP/BZA/H<sub>2</sub>O mixtures:



These transformations were reversible upon cooling. NMR results<sup>4</sup> indicate that a lamellar phase coexists with what we term the  $R_\alpha$  and  $Rb_\alpha$  phases. We can infer that a separate lamellar phase exists in which it must have the same repeat spacing as one of the rectangular axes. Diffraction patterns of the full temperature scan for sample B2 upon heating are shown in Figure 4. The x-ray patterns obtained between 46.6 and 47.7°C (frames 103 to 112) for sample B2 are superpositioned on Figure 5 to show that the  $L_\beta$  to  $L_\alpha$  phase transition as indicated by the elimination of the wide angle peak occurs without a change in the small angle scattering pattern of the  $Rb_\alpha$  phase. The  $Rb_\alpha$  to  $L_\alpha$  transition occurs at an even higher temperature. Diffraction patterns of the full temperature scan for sample B1 upon cooling are

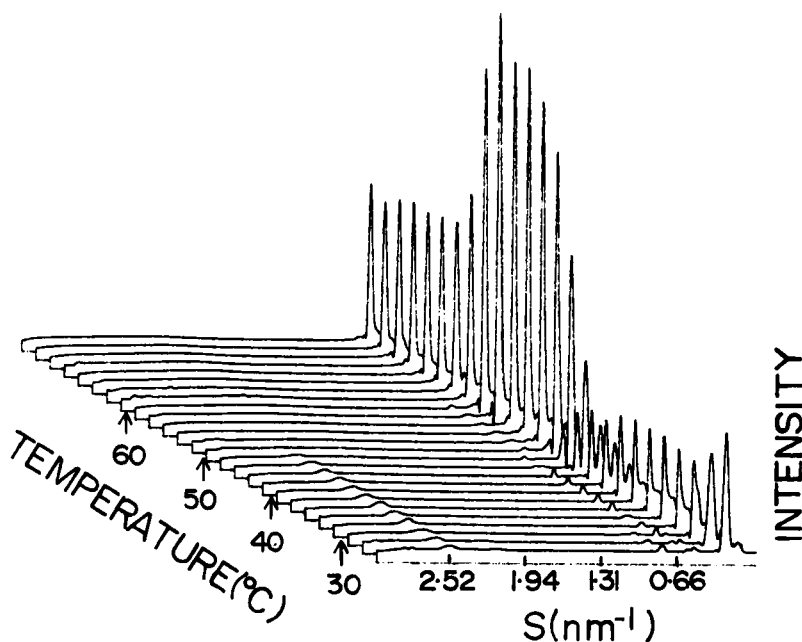


FIGURE 4 X-ray diffraction patterns of a 66.5%/1.1%/32.4% mixture by weight of potassium palmitate/benzoyl alcohol/water collected every 1.2 s as the sample is heated at  $10^\circ\text{C min}^{-1}$ . The intensity is plotted as a function of reciprocal space. Every tenth frame is shown in this figure.

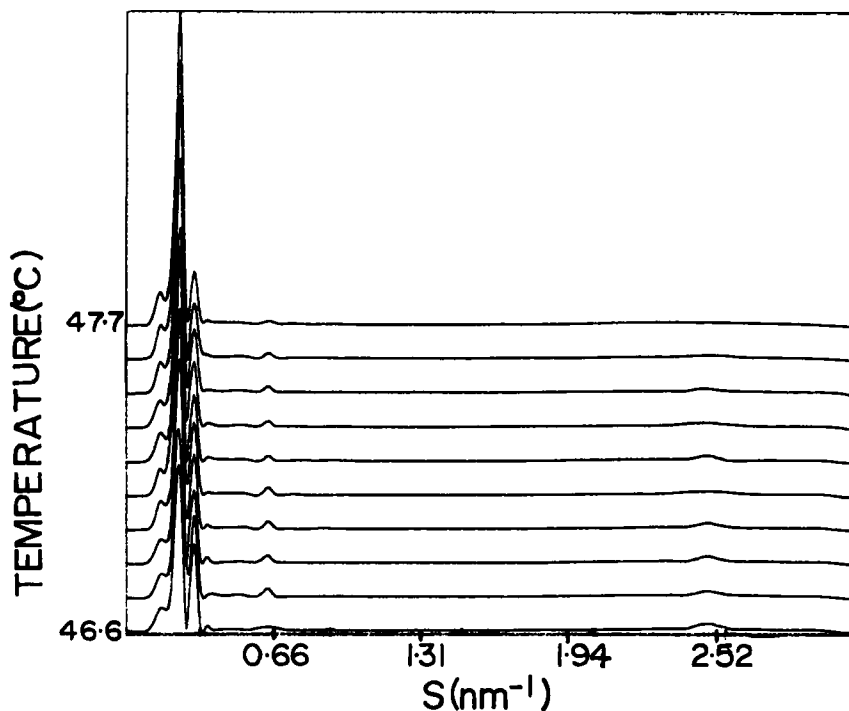


FIGURE 5 X-ray diffraction patterns recorded between 46.6 and 47.7°C from the data set in Figure 4.

shown in Figure 6. Diffraction patterns from 31.4 to 25.7°C (i.e., frames 220 to 240) are superpositioned in Figure 7 to show that the  $Rb_\alpha$  to  $R_\alpha$  transition precedes the  $L_\beta$  to  $L_C$  transition upon cooling for sample B1. It is relevant to note that there was little hysteresis in the lamellar phases upon cooling for these samples and that the dimensions of the a and b axes and the diagonal axes remain constant for continuous transitions involving the rectangular or ribbon phases.

## DISCUSSION

Lyotropic liquid crystals made from surfactants have historically been the object of much interest because of the vast array of phases present and the complexity of the transformation between phases. The presence of high luminescent x-ray beams at synchrotron sources allows one to obtain high resolution x-ray diffraction patterns in these systems in seconds or less. We have therefore been able to characterize the structures involved in the phase transformations in the mixed surfactant systems of KP/KL/H<sub>2</sub>O and KP/BZA/H<sub>2</sub>O, and to provide structural evidence in these systems for the existence of ribbon phases—deformed cylinders packed in a rectangular unit cell. These interpretations were correlated to the NMR findings of Doane and co-workers.<sup>4–7,21</sup> In addition, we have determined that the

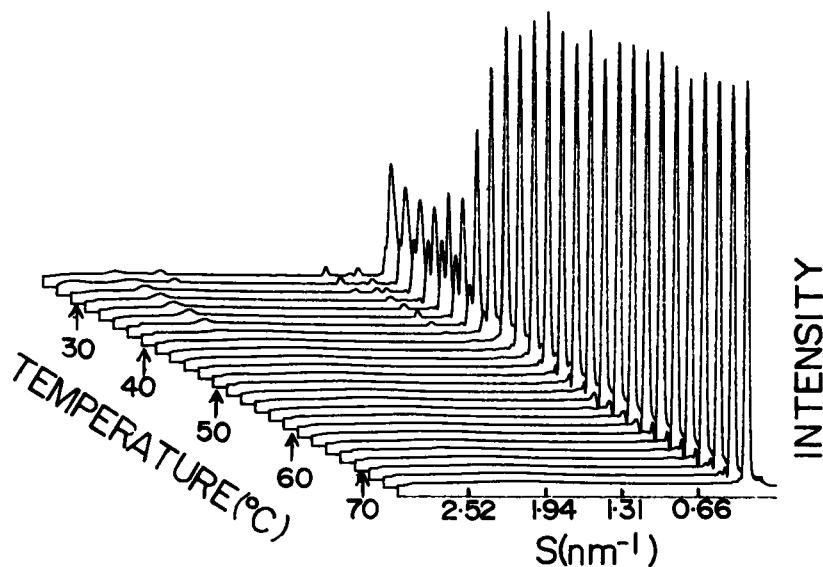


FIGURE 6 X-ray diffraction patterns of a 64.3%/3.9%/31.8% mixture by weight of potassium palmitate/benzoyl alcohol/water collected every 1–2 s as the sample is cooled at  $10^{\circ}\text{C min}^{-1}$ . The intensity is plotted as a function of reciprocal space. Every tenth frame in the data set is shown in this figure.

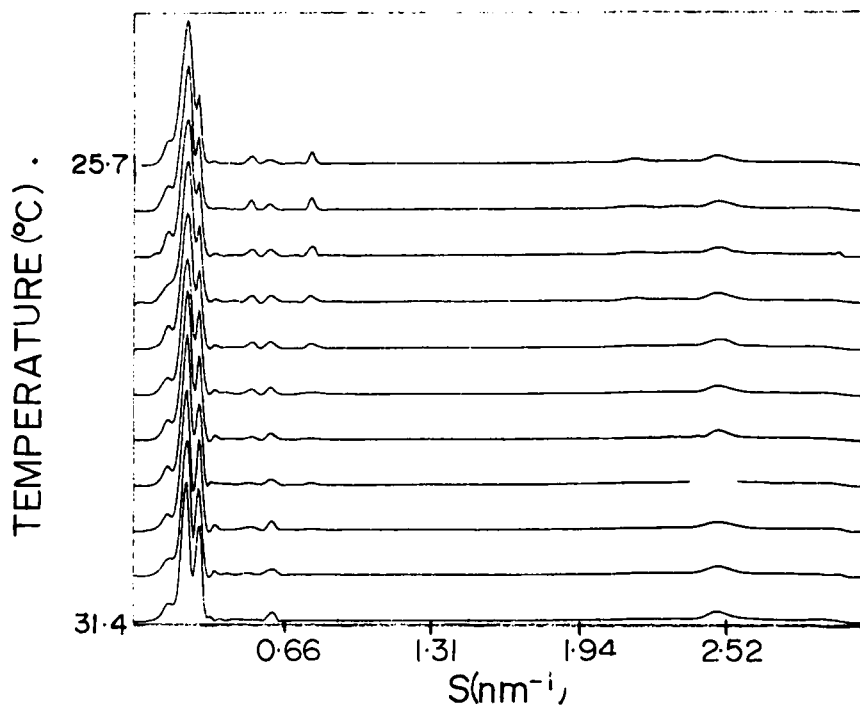


FIGURE 7 X-ray diffraction patterns recorded between 31.4 and  $25.7^{\circ}\text{C}$  for the data set in Figure 6.

low temperature coexisting lamellar phase has a crystalline or subgel acyl chain packing structure.

Time resolved x-ray diffraction studies are useful in determining phase transition mechanisms, kinetics and hysteresis. The hysteresis in the lamellar acyl chain packing and rectangular mesophase dimensions observed on cooling various KP/KL/H<sub>2</sub>O mixtures does not appear as a direct function of changing the KP/KL weight ratio in a uniform manner. Rather, individual mixtures may exhibit an hysteretic phenomenon in the mesophase and/or subcell structure. Preliminary experiments on approximately ten KP/KL/H<sub>2</sub>O mixtures (L. J. Lis and P. J. Quinn, unpublished observation) showed similar apparently random hysteretic behavior. Until a general trend is observed, all KP/KL/H<sub>2</sub>O samples must be rigorously prepared and characterized for hysteresis. It would appear that the interesting phase behavior can also be examined in similar systems without hysteresis affecting measurements recorded during various thermal cycles (i.e., KP/BZA/H<sub>2</sub>O). It may be preferable to restrict detailed studies to these less sensitive systems.

Although the KP/KL/H<sub>2</sub>O mixtures appear to have a uniform phase behavior which is unaffected by large changes in the KP/KL weight ratio, the KP/BZA/H<sub>2</sub>O phase behavior is drastically changed as the weight percentage of BZA increases from ~1 to ~3% with an equivalent drop in the KP weight percent. However, a trend can be determined for the effect of increasing BZA in these mixtures. Specifically, as the percentage of BZA increases (1) the temperature of the transition between the lamellar gel and lamellar liquid-crystalline phases decreases, and (2) the temperature of the ribbon liquid-crystalline to lamellar liquid-crystal phases decreases. We can infer that the presence of BZA perturbs the order within the surfactant lamellar mesophase packing array (much as it does in lipid bilayers) although not sufficiently to cause the formation of a gel rather than subgel low temperature acyl chain packing. This change in packing order also allows the lamellar gel phase to be stable at higher temperatures and low BZA contents before transforming into the lamellar liquid-crystalline phase. In addition, the ribbon phase appears to become more stable at high temperature for all BZA contents since it transforms into the liquid-crystalline bilayer state after the coexisting bilayer phase does. This is in contrast to the KP/KL/H<sub>2</sub>O system where both phases transform into the  $L_\alpha$  phase within a few degrees.

### Acknowledgments

This work was partially supported by a grant from the Science and Engineering Research Council (SERC), U.K. (P. J. Q.).

### References

1. V. Luzzati, in *Biological Membranes* (D. Chapman, ed.), Academic Press, pp. 71–123 (1968).
2. S. Friberg (ed.), *Adv. Chem. Series 152*, American Chemical Soc., Washington, D.C., 156 pp., 1976.
3. R. M. Wood and M. P. McDonald, *J. Chem. Soc. Faraday Trans. 1* **81**, 273–283, (1985).
4. G. Chidichimo, N. A. P. Vaz, Z. Yaniv and J. W. Doane, *Phys. Rev. Letters* **49**, 1950–1954 (1982).

5. J. W. Doane, G. Chidichimo and A. Golemme, *Mol. Cryst. Liq. Cryst.* **113**, 25–36 (1984).
6. G. Chidichimo, A. Golemme, J. W. Doane and P. W. Westerman, *J. Chem. Phys.* **82**, 536–540 (1985).
7. G. Chidichimo, A. Golemme, G. A. Ranieri, M. Terenzi and J. W. Doane, *Mol. Cryst. Liq. Cryst.* **132**, 275–288 (1986).
8. Y. Hendrikx and J. Charvolin, *J. Phys. (Paris)* **42**, 1427–1440 (1981).
9. B. G. Tenchov, L. J. Lis and P. J. Quinn, *Biochim. Biophys. Acta* **897**, 143–151 (1987).
10. A. Sen, D. A. Mannock, D. G. Collins, P. J. Quinn and W. P. Williams, *Proc. Roy. Soc. Lond.* **B218**, 349–364 (1983).
11. M. J. Ruocco and G. G. Shipley, *Biochim. Biophys. Acta* **691**, 309–320 (1982).
12. J. M. Seddon, K. Harlos and D. Marsh, *J. Biol. Chem.* **258**, 3850–3854 (1983).
13. H. H. Mantsch, S. C. Hsi, K. W. Butler and D. G. Cameron, *Biochim. Biophys. Acta* **728**, 325–330 (1983).
14. S. Mulukutla and G. G. Shipley, *Biochemistry* **23**, 2514–2519 (1984).
15. L. J. Lis and P. J. Quinn *Mol. Cryst. Liq. Cryst.* **140**, 319–325 (1986).
16. C. Nave, J. R. Helliwell, P. R. Moore, A. W. Thompson, J. S. Morgan, R. J. Greenall, A. Miller, S. K. Bailey, J. Bradshaw, W. J. Pigram, W. Fuller, D. P. Seddons, M. Deutsch and R. T. Tregear, *J. Appl. Cryst.* **18**, 396–403 (1985).
17. J. R. Helliwell, T. J. Greenough, P. D. Garr, S. A. Rule, P. R. Moore, A. W. Thompson and J. S. Morgan, *J. Phys.* **E15**, 1363–1372 (1982).
18. C. W. Bunn and E. B. Howells, *Nature (London)* **174**, 549–551 (1954).
19. Y. K. Levine, *Prog. Surf. Sci.* **3**, 279–352 (1973).
20. P. K. T. Persson, *Chem. Phys. Lipids* **34**, 287–299 (1984).
21. J. M. Pope and J. W. Doane, *J. Chem. Phys.* **87**, 3201–3206 (1987).